Increase in Thiol Oxidative Stress via Glutathione Reductase Inhibition as a Novel Approach to Enhance Cancer Sensitivity to X-Ray Irradiation

Yong Zhao[1], **Teresa Seefeldt**[2], **Wei Chen**[2], **Laura Carlson**[2], **Adam Stoebner**[2], **Sarah Hanson**[2], **Ryan Foll**[2], **Duane P. Matthees**[3], **Srinath Palakurthi**[4], and **Xiangming Guan**[2]

[1] Department of Physiology, Michigan State University, East Lansing, MI 48824

[2] Department of Pharmaceutical Sciences, South Dakota State University, Brookings, SD 57007

[3] Department of Veterinary Science, South Dakota State University, Brookings, SD 57007

[4] Irma Lerma Rangel College of Pharmacy, Texas A&M Health Science Center Kingsville, TX 78363

Abstract

Depletion of reduced form glutathione (GSH) has been extensively studied for its effect on sensitizing cancer to radiation. However, little is known about the effect of thiol oxidative stress created through an increase in glutathione disulfide (GSSG) on cancer sensitivity to radiation. In this study, an increase in GSSG was effectively created by 2-acetylamino-3-[4-(2-acetylamino-2-carboxyethylsulfanylthiocarbonylamino)phenylthiocarbamoylsulfanyl]propionic acid (2-AAPA), an irreversible glutathione reductase (GR) inhibitor. Our results demonstrate that the GSSG increase significantly enhanced cancer sensitivity to X-ray irradiation in four human cancer cell lines (A431, MCF7, NCI-H226 and OVCAR-3). When cells were pretreated with 2-AAPA followed by X-ray irradiation, the IC_{50} values of X-ray for A431, MCF7, NCI-H226 and OVCAR-3 cells were reduced from 24.2±2.8, 42.5±3.0, 43.0±3.6 and 27.8±3.5 Gy to 6.75 ±0.9, 8.1±1.1, 6.75±1.0, and 12.1±1.7 Gy respectively. The synergistic effects observed from the combination of X-ray plus 2-AAPA were comparable to that from the combination of X-ray plus buthionine sulfoximine (BSO), a reference compound known to increase cancer sensitivity to radiation. The synergistic effect was correlated with an increase in cell thiol oxidative stress which was reflected by a 5–6 fold increase in GSSG and 25% increase in total disulfides. No change in GSH and total thiols was observed as a result of GR inhibition.

Keywords

Thiol oxidative stress; glutathione disulfide (GSSG); disulfides; glutathione reductase; cancer radiotherapy sensitivity

To whom correspondence should be addressed: Xiangming Guan, Ph.D., South Dakota State University, College of Pharmacy, Box 2202C, Brookings, SD 57007. Tel.: (605) 688-5314; Fax: (605) 688-5993. Xiangming.Guan@sdstate.edu.

Introduction

Radiotherapy is one of the major therapies for cancer treatment. Radiotherapy produces cancer cell growth inhibition by generating free radicals which, in turn, cause DNA breaks and damage to other cellular components [1]. One of the major issues associated with clinical use of radiotherapy is the development of radiotherapy resistance [2]. The mechanisms by which tumor cells develop radiation resistance are complex and can be due to local tissue hypoxia, over expression of antioxidant enzymes such as catalase, superoxide dismutase (SOD), glutathione peroxidase (GP), and glutathione reductase (GR), over production of antioxidants, primarily thiols, and inherent factors such as p53 status and bcl-2 activity [1,3–18].

Several pharmacologically based approaches have been successfully employed to reduce radiotherapy resistance. Specifically, these approaches include modulation of the intracellular thiol pool, blockage of bcl-2, inhibition of topoisomerase II or activated Ras, and a combination of radiation with antiangiogenesis agents [7–13,15–16,19–23].

Thiols play an important role in cancer resistance to radiotherapy. The mechanism of cancer resistance caused by thiols is attributed to the ability of thiols to terminate free radicals. Glutathione (GSH) is the most prevalent non-protein thiol (NP-SH) in mammalian cells. GSH terminates free radicals with itself being oxidized to glutathione disulfide (GSSG) (Scheme 1). Due to the relevance of GSH in terminating free radicals, numerous reports have been documented about the effects of GSH depletion on cancer sensitivity to radiation and other chemotherapeutic treatments [8,24]. The most extensively studied GSH depletion agent is buthionine sulfoximine (BSO), an inhibitor of the rate determining enzyme γ-glutamylcysteine synthetase in GSH biosynthesis. BSO has been demonstrated to effectively deplete GSH and sensitize cancer to radiation [25–30] and other chemotherapeutic agents [8,24].

Another enzyme related to GSH metabolism is glutathione reductase (GR, EC 1.8.1.7). GR catalyzes the reduction of GSSG back to GSH to maintain a reducing intracellular environment (Scheme 1) [9,31]. Inhibition of this enzyme has been demonstrated to lead to an accumulation of GSSG creating a state of thiol oxidative stress [32,33]. However, studies about the effect of thiol oxidative stress created through an increase in GSSG on cancer sensitivity to radiation are limited. Recently, Coleman and coworkers demonstrate that 2- deoxy-D-glucose increased GSSG levels by blocking glucose metabolism and sensitized pancreatic cancer to radiation [34]. It needs to be noted that thiol oxidative stress created through an increase in GSSG is not the same as thiol oxidative stress created through depletion of GSH. Further, considering the ratios of GSH/GSSG which range from 30:1 to 300:1 with typical intracellular GSH in millimolar concentrations [35,36], an increase in GSSG is expected to produce more significant impact on the thiol redox potential than depletion of GSH. In this investigation, the effect of an increase in thiol oxidative stress through an accumulation of GSSG on cancer sensitivity was examined in four human cancer cell lines (A431, MCF7, NCI-H226 and OVCAR-3). The accumulation of GSSG was achieved by the use of 2-acetylamino-3-[4-(2-acetylamino-2-carboxyethylsulfanyl-thiocarbonylamino)phenylthiocarbamoylsulfanyl]propionic acid (2-AAPA), a selective and irreversible GR inhibitor with K_i and k_{inact} values of 56 μM and 0.1 min^{-1} respectively [37]. 2-AAPA did not cause any significant change in GSH in this study. This study also employed BSO as a reference compound. Our data demonstrate that cancer cells became more sensitive to radiation when they were pretreated with 2-AAPA to create a state of thiol oxidative stress. The synergistic effect observed for the combination of 2-AAPA and radiation were comparable to that observed from the combination of BSO and radiation. The sensitizing effect was correlated with an increase in cell thiol oxidative stress which was reflected by a 5–6 fold increase in GSSG and 25% increase in total disulfides which include protein disulfides and non-protein disulfides.

Materials and Methods

Materials

GSH, GSSG, 5,5′-dithiobis(2-nitrobenzoic acid) (DTNB, Ellman's reagent), sodium borohydride ($NaBH_4$), BSO, *p*-aminobenzoic acid, β-methylphenylalanine, sulfosalicylic acid, dimethyl sulfoxide (DMSO), ethylenediamine tetraacetic acid (EDTA), bovine serum albumin (BSA), insulin, and Bradford reagent were obtained from Sigma-Aldrich Chemical Co. (Milwaukee, WI). MEM and RPMI 1640 growth medium, fetal bovine serum (FBS), penicillin/ streptomycin, and phosphate buffered saline (PBS) were purchased from Mediatech, Inc (Herndon, VA). DMEM growth medium was bought from the American Type Culture Collection (ATCC, Bethesda, MD). 2-AAPA was obtained through a one-step synthesis from commercially available starting materials [37]

Stock solutions

Solutions of DTNB, *p*-aminobenzoic acid, and $NaBH_4$ were made in 0.15 M NaH_2PO_4 (pH 7.5). Solutions of GSH, GSSG, and β-methylphenylalanine were prepared in 0.1% HCl aqueous solution. 2-AAPA (2 mM) was dissolved in DMEM, MEM, or RPMI 1640 growth medium containing 10% FBS and 1% penicillin/streptomycin. BSO (20 mM) was made in ultrapure water (Milli-Q purification system, Millipore, Bedford, MA) with pH adjusted to 10. Stock solutions of 2-AAPA and BSO were filtered through a Medical Millex-GP Filter (0.22 μm, sterilized, Millipore, Billerica, MA). All stock solutions were stored at −80°C before use except $NaBH_4$ which was prepared fresh and stored over ice for one-day assay. The stock solutions of 2-AAPA and BSO were diluted to the concentration needed for treatment of cells with DMEM, MEM or RPMI 1640 growth medium.

Part 1. Determination of Cancer Sensitivity to Radiation

Cell lines and culture—A431 (human skin cancer cell line) and MCF7 (human breast cancer cell line) were obtained from American Type Culture Collection (ATCC, Manassas, VA). NCI-H226 (human lung cancer cell line) and OVCAR-3 (human ovarian cancer cell line) were obtained from the National Cancer Institute. The cells were maintained in DMEM (A431), MEM (MCF7) or RPMI 1640 (NCI-H226 and OVCAR-3) growth medium containing 10% FBS and 1% penicillin/streptomycin in a humidified atmosphere consisting of 5% CO_2 at 37° C. Insulin (10 μg/mL) was added as an additional component in the MEM medium for MCF7 cells.

Cell viability—Cell viability was measured by a colorimetric assay in a 96-well plate with MTT (3-[4,5]-dimethylthiazol-2, 5-diphenyltetrazolium bromide) [38]. Briefly, at the end of cell growth, the medium was removed and replaced with an MTT solution (0.5 mg/mL, 50 μL/well). The plate was protected from light and incubated at 37°C for 4h in a humidified atmosphere of 5% CO_2. A purple formazan product was then formed by the action of mitochondrial enzymes in metabolically viable cells. This product was dissolved by DMSO (150 μL/well, 1h). The absorbance of each well was quantified with a SpectraMax M2 microplate reader (Molecular Devices, Sunnyvale, California) using a test wavelength of 570 nm and a reference wavelength of 650 nm.

Determination of X-ray irradiation dose response curves—To determine the effect of X-ray irradiation alone on the viability of the cancer cell lines, a dose response curve was determined with each cell line. Exponentially growing cells were plated at a density based on the optimal cell numbers obtained for each cell line (1000 cells/well for A431, 2500 cells/well for MCF7, 1800 cells/well for NCI-H226, and 1500 cells/well for OVCAR-3) in 96-well plates. The cells were allowed to attach for 24h at 37°C in a humidified atmosphere of 5% CO_2. After 24h, the medium was removed and replaced with fresh medium. Radiation was carried out

using a Cabinet X-ray system-Faxitron Series (Model RX-650, Faxitron X-ray Corp, Wheeling, IL). A lead plate was employed to assure that radiation was delivered only to the intended column. Dosages from 6.75 to 101.25 Gy were delivered at a rate of 6.75 Gy/min with the following settings: 130 kVp, 5 mA, and 0.5 mm aluminum filter. After radiation, the 96-well plate was returned to the incubator for an additional 6 days. Cell viability was determined by the MTT assay. A control experiment was conducted in parallel with no radiation applied. It needs to be noted that the radiation dosage indicated is the dosage delivered from the X-ray machine to the 96-well plate with the plate lid on. The IC_{50} of radiation for each cell line was derived from the dose-response curve. The IC_{50} is defined as the dose of X-ray that inhibits cell growth by 50%.

Determination of 2-AAPA dose response curves—To determine the effect of 2-AAPA alone on the viability of the cancer cell lines, the dose response curve of 2-AAPA for each cell line was obtained, and from which the IC_{50} value of 2-AAPA was derived. The determination followed the same procedure as described for the X-ray dose response curves except the cells were treated with 2-AAPA (1 μM to 1000 μM) instead of radiation. A control experiment was carried out in parallel with no 2-AAPA treatment.

Determination of the effect of 2-AAPA on cancer cell sensitivity to X-ray irradiation—Exponentially growing cells were plated as described above, and the cells were allowed to attach for 24h at 37°C in a humidified atmosphere of a 5% CO_2 incubator. After the attachment period, the medium was removed and replaced with medium containing 2-AAPA. After a 2h treatment with 2-AAPA, X-ray irradiation was carried out as described above, and the cells were allowed to grow for an additional 6 days at 37°C in a humidified atmosphere of a 5% CO_2 incubator. Cell viability was determined by the MTT assay. A control experiment was carried out in the same way except cells were treated with no 2-AAPA or X-ray irradiation.

Determination of the effect of BSO on cancer cell sensitivity to X-ray irradiation —Exponentially growing cells were plated and allowed to attach as described above. After the attachment period, the medium was removed and replaced with medium containing BSO (50 μM), and the cells were incubated in the incubator for 24h before X-ray irradiation. X-ray irradiation was carried out as described above, and the cells were allowed to grow for an additional 5 days (total incubation length was the same as that in the treatment with 2-AAPA). Cell viability was determined as described above. A control experiment was carried out in the same way except cells were treated with no BSO or X-ray irradiation.

Synergism calculation—The synergism of 2-AAPA and X-ray irradiation was calculated based on a method described by Momparler [39]. An expected value of cell survival rate (S_{exp}) is defined as the product of the survival rates observed from 2-AAPA (S_{2-AAPA}) and X-ray (S_{X-ray}): $S_{exp} = S_{2-AAPA} \times S_{X-ray}$. The synergistic effect, S_{syn}, is defined as the result when the observed survival rate (S_{obs}) from the combination treatment is lower than S_{exp} ($S_{exp} - S_{obs} > 0$). When $S_{exp} - S_{obs} = 0$ or < 0, it is defined as an additive or antagonistic effect, respectively. A synergistic effect is expected if 2-AAPA increases the sensitivity of cancer cells to radiation.

Part 2. Determination of GR Activity, GSH, GSSG, Total Thiols and Total Disulfides in OVCAR-3 Cells

Cell treatment—Exponentially growing OVCAR-3 cells (2.5 million in 58.5 mL growth medium) were placed in a 185 cm^2 flask under the same culture conditions described above for 24h for attachment. After attachment, the flask was added with 1.5 mL of the stock solution of 2-AAPA (2 mM) to give the final concentration of 50 μM (for 2-AAPA alone and the

combination of 2-AAPA plus X-ray) or with 1.5 mL of fresh medium (for control and X-ray alone). The cells were then incubated for 2h. Following this incubation, the cells for the X-ray treatment and X-ray plus 2-AAPA were exposed to X-ray irradiation at a dose of 13.5 Gy. All of the flasks were then incubated for an additional 30 minutes. At the end of each treatment, the total number of cells in each flask was about 5 million. The medium was then collected, and the cells were rinsed with PBS and detached by trypsinization. The medium and the cell suspension were combined and centrifuged at $1000 \times g$ for 5 min. The cell pellet from each flask was collected and then divided for the following assays: ~2 million cells for the determination of GR activity and protein content and ~3 million cells for quantification of GSH, GSSG, total thiol, and total disulfides. Protein content was determined by the Bradford method with BSA as the standard (Sigma-Aldrich Co., Milwaukee, WI). Cell viability was determined by trypan blue staining.

Determination of GR activity—The cell pellet obtained above was washed with ice-cold PBS containing 1 mM EDTA (5 mL), then suspended in 0.4 mL of hypotonic phosphate buffer (1 mM, pH 7.5) containing 1 mM EDTA, and sonicated using a Misonix XL2020 sonicator with a cup horn probe (Farmingdale, NY) for 4 min. The homogenate was centrifuged at $120,000 \times g$ for 20 min at 4°C, and GR activity in the supernatant was determined as described [40]. Briefly, the assay mixture contained the supernatant (300 μL), BSA (1 mg/mL), and NADPH (0.2 mM). The enzymatic reaction was initiated by addition of GSSG (0.52 mM). GR activity was measured by the initial rates of disappearance of NADPH determined spectrophotometrically at λ=340 nm.

Preparation of cell lysate for quantification of GSH, GSSG, total thiols and total disulfides—The cell pellet was washed with 5 mL ice-cold PBS containing 1 mM EDTA, then suspended in 0.5 mL of 10% sulfosalicylic acid, and sonicated using a Misonix XL2020 sonicator with a cup horn probe (Farmingdale, NY) for 4 min.

Quantification of GSH and GSSG—GSH and GSSG were quantified as described previously with minor modification [41]. Briefly, the cell lysate (100 μL) prepared above was added with β-methylphenylalanine (100 μg/mL, 10 μL) as an internal standard and DTNB (50 mM, 60 μL), followed by neutralization with phosphate buffer (0.5 M, pH 10, 200 μL) (final pH 7.4). The samples were left at ambient temperature for 15 min to allow the completion of GSH derivatization by DTNB. After derivatization, the samples were acidified by HCl (10 M, 30 μL), and the acidified samples were diluted 10 times with 0.1% HCl solution. Fifty μL of the diluted sample was injected into LC/MS for quantification of GSSG and the derivatized GSH. Standard curves were constructed by spiking the cell lysate with various known amounts of GSH (for GSH quantification) or GSSG (for GSSG quantification). The LC/MS analysis was conducted on a Waters Micromass Quattro Ultima Mass Unit (Waters, Milford, MA).

Quantification of total thiols and total disulfides—Quantification of total thiols, which include protein thiols and non-protein thiols, and total disulfides followed a procedure developed recently from this laboratory [42]. The method was based on the HPLC quantification of TNB released from the reaction of DTNB with thiols before and after $NaBH_4$ reduction of disulfides.

Statistical Analysis—Data were analyzed using statistical functions in Microsoft Excel and are shown as means ±S.D. Student *t*-tests were performed for significance of differences in sample means with a cutoff of $p < 0.05$.

Results and Discussion

Thiol redox buffer, reflected by the ratio of GSH/GSSG, is the principal redox buffer of the cell [35,43]. The high ratio of GSH/GSSG, the basis of the intracellular reducing environment, is primarily maintained by GR through reduction of GSSG back to GSH [44]. Inhibition of GR leads to an accumulation of GSSG which increases intracellular thiol oxidative stress. As a result, the cells are likely to be more susceptible to damage caused by oxidative stress. Consistently, an increase in GR activity has been found to attribute to the resistance to radiotherapy [5,7,9]. Therefore, it is reasonable to expect that an increase in cellular thiol oxidative stress through inhibition of GR would make cancer cells more susceptible to oxidative stress damage incurred by radiation.

In this study, 2-AAPA, a novel dithiocarbamate GR inhibitor, was used as a tool to investigate the effect of GR inhibition on the sensitivity of cancer cells to X-ray irradiation. Initially, N,N-bis(2-chloroethyl)-N-nitrosourea (BCNU), the most commonly used irreversible GR inhibitor with an IC_{50} value of 647 μM against yeast GR [45], was employed for the investigation. However, the DNA alkylating property of BCNU [45] complicates its use as a GR inhibitor for this investigation. 2-AAPA, employed in this study, was identified as a selective irreversible GR inhibitor and is able to create a state of thiol oxidative stress through accumulation of GSSG with minimal impact on other cellular functions [37]. Four human cancer cell lines were selected in the study. These cell lines have been used in studies examining methods of increasing cancer sensitivity to radiation [3,25,46,47]. BSO was used as a reference compound as it has been shown to increase cancer sensitivity to radiation through depletion of GSH [48]. In addition BSO has been in clinical trials to evaluate its sensitizing effect in cancer patients [49].

Based on the dose-response curves (Figure 1), the IC_{50} values of X-ray for A431, MCF7, NCI-H226 and OVCAR-3 cells were determined to be 24.2±2.8, 42.5±3.0, 43.0±3.6 and 27.8±3.5 Gy respectively. To find an optimal concentration for the study of cancer sensitizing effect, dose-response curves of 2-AAPA were obtained. Our results show that 2-AAPA itself did produce cytotoxicity against A431, MCF7, NCI-H226 and OVCAR-3 cells with average IC_{50} values of 73.1±4.0 μM, 75.2±5.2 μM, 68.4±4.3 μM and 68.1±5.2 μM, respectively. It is not clear whether the cytotoxicity of 2-AAPA is related to the inhibition of GR. To determine the effect of GR inhibition on cancer sensitivity, cancer cells were pretreated with 2-AAPA for 2 hours followed by X-ray radiation. Table 1 shows observed cell survival rates (S_{obs}), expected cell survival rates (S_{exp}), and synergistic effect obtained from drug combinations of 2-AAPA at different concentrations plus a fixed radiation dosage. The fixed radiation dosage was selected in a way that the dosage would produce some cell death but also provide enough space to observe synergistic effects. Based on these results, the concentrations of 2-AAPA found to produce the best synergistic effects with X-ray radiation were determined to be 55 μM, 60 μM, 60 μM and 50 μM for A431, MCF7, NCI-H226 and OVCAR-3, respectively (Table 1). Concentrations of 2-AAPA higher than these concentrations caused too much cell death and did not give enough space to observe synergistic effects (data not shown). These concentrations were then selected to investigate the effect of 2-AAPA on the sensitivity of the cancer cell lines to X-ray radiation. Table 2 presented S_{obs}, S_{exp} and synergistic effects obtained from drug combinations of a fixed concentration of 2-AAPA plus X-ray radiation at different dosages. The results reveal that 2-AAPA produced synergistic effects with X-ray radiation at most employed dosages in all four cell lines studied demonstrating that 2-AAPA effectively increased the sensitivity of the cancer cells to radiation (Table 2). The highest synergistic effects produced by the combination of 2-AAPA and X-ray were 11.8±1.9%, 11.5±2.4%, 11.5±2.3%, and 16.7±1.6% respectively with A431, MCF7, NCI-H226 and OVCAR-3 cell lines (Table 2). The effects of 2-AAPA at the optimal concentration on the dose-response curves of X-ray radiation with the four cancer cell lines are presented in Figure 1. Based on the dose-responses

curves, the IC_{50} values of X-ray for A431, MCF7, NCI-H226 and OVCAR-3 cells were reduced from 24.2±2.8, 42.5±3.0, 43.0±3.6 and 27.8±3.5 Gy to 6.75 ±0.9, 8.1±1.1, 6.75±1.0, and 12.1 ±1.7 Gy respectively (Figure 1). To place 2-AAPA's effect on cancer radiation sensitizing effect in a perspective, the effect of BSO on radiation sensitivity in these four cell lines was determined. Table 3 presents S_{obs}, S_{exp}, and synergistic effect obtained from the combination of X-ray radiation at different dosages plus BSO at 50 μM, a concentration used in the literature to increase cancer cell sensitivity to radiation (48). As shown in table 3, synergistic effects were observed from all the drug combinations studied demonstrating that BSO effectively increased the sensitivity of these cancer cells to radiation. The highest synergistic effects produced by BSO were found to be 15.3±2.1%, 14.7±1.2%, 14.5±1.5%, 22.4±2.3% respectively with A431, MCF7, NCI-H226 and OVCAR-3 cell lines (Table 3). BSO reduced the IC_{50} values of X-ray to 16.3 ±2.8, 26.7±2.3, 19.5 ±1.9, and 17.3 ±2.1 Gy respectively for A431, MCF7, NCI-H226 and OVCAR-3 cell lines. It needs to be noted that although 2-AAPA reduced IC_{50} more significantly than BSO based on the dose-response curves, 2-AAPA produced more cytotoxicity than BSO at the concentration employed (Tables 2 and 3). Nevertheless, the synergistic effects produced by the combination of 2-AAPA and X-ray radiation are comparable to that obtained from the combination of BSO and X-ray radiation.

To examine whether the synergistic effect is correlated with thiol oxidative stress, intracellular GR, GSH, GSSG, total thiols and total disulfides were determined in OVCAR-3 cells, the cell line where the best synergistic effect was observed for the combination of 2-AAPA and X-ray. As expected, at the end of a two hour treatment with 50 μM 2-AAPA, 80±3% of GR activity was inhibited (Figure 2). Consistently, an increase in GSSG was observed. GSSG was increased by 2–3 fold after treatment with 2-AAPA (50 μM) for 2h (Figure 3A). Interestingly, compared with the control, no significant decrease in GSH was observed by GR inhibition (Figure 3B), which is not totally unexpected considering the relatively low quantity of GSSG compared to that of GSH in cells and that inhibition of GR may not produce too much impact on the GSH level. Nevertheless, the increase in GSSG indicates a state of thiol oxidative stress. On the other hand, radiation alone (13.5 Gy) did not produce any significant effect on GR (Figure 2), GSSG (Figure 3A) or GSH (Figure 3B). However, when cells were pretreated with 2-AAPA (50 μM) for 2h followed by X-ray radiation (13.5 Gy), GSSG was increased 5–6 fold compared with only a 2–3 fold increase by 2-AAPA alone and no change from radiation alone indicating that the oxidatively stressed cells were more susceptible to radiation insult (Figure 3A). Similarly, a significant increase in the content of total disulfides was only noticed in the cells pretreated with 2-AAPA followed by radiation (Figure 3D). As noticed with GSH, no significant changes were found in the content of total thiols by 2-AAPA, radiation, or a combination of 2-AAPA and radiation (Figure 3C) revealing that GR inhibition showed a minimal impact on the levels of thiols despite the increase in disulfides. Overall these results suggest that an increase in thiol oxidative stress was likely to be the mechanism behind the observed synergistic effect of X-ray and 2-AAPA.

Together, these data demonstrate that an increase in thiol oxidative stress through inhibition of GR can increase cancer cell sensitivity to radiation. The increase in sensitivity was comparable to that produced by BSO. Further *in vivo* investigation is needed to evaluate its potential as a novel approach to increase cancer sensitivity to radiation.

Acknowledgments

Abbreviations

2-AAPA

2-acetylamino-3-[4-(2-acetylamino-2-carboxyethylsulfanylthio-carbonylamino)phenylthiocarbamoylsulfanyl]propionic acid

BCNU

N,N-bis(2-chloroethyl)-*N*-nitrosourea

BSO

buthionine sulfoximine

DTNB

5,5′-dithiobis(2-nitrobenzoic acid)

GP

glutathione peroxidase

GR

glutathione reductase

GSH

Reduced form glutathione

GSSG

oxidized form glutathione or glutathione disulfide

NaBH$_4$

sodium borohydride

SOD

superoxide dismutase

References

1. Belka C. The fate of irradiated tumor cells. Oncology 2006;25:969–971.

2. Fitzgerald TJ, Wang T, Goel HL, Huang J, Stein G, Lian J, Davis RJ, Doxsey S, Balaji KC, Aronowitz J, Languino LR. Prostate carcinoma and radiation therapy: therapeutic treatment resistance and strategies for targeted therapeutic intervention. Expert Rev Anticancer Ther 2008;8:967–974. [PubMed: 18533806]

3. Wang T, Tamae D, LeBon T, Shively JE, Yen Y, Li J. The role of peroxiredoxin II in radiation-resistant MCF-7 breast cancer cells. Cancer Res 2005;65:10338–10346. [PubMed: 16288023]

4. Hirose K, Longo DL, Oppenheim JJ, Matsushima K. Overexpression of mitochondrial manganese superoxide dismutase promotes the survival of tumor cells exposed to interleukin-1, tumor necrosis factor, selected anticancer drugs, and ionizing radiation. FASEB J 1993;7:361–368. [PubMed: 8440412]

5. Sun J, Chen Y, Li M, Ge Z. Role of antioxidant enzymes on ionizing radiation resistance. Free Radic Biol Med 1998;24:586–593. [PubMed: 9559871]

6. Suresh A, Tung F, Moreb J, Zucali JR. Role of manganese superoxide dismutase in radioprotection using gene transfer studies. Cancer Gene Ther 1994;1:85–90. [PubMed: 7621245]

7. Bump EA, Brown JM. Role of glutathione in the radiation response of mammalian cells in vitro and in vivo. Pharmacol Ther 1990;47:117–136. [PubMed: 2195553]

8. Meister A. Glutathione deficiency produced by inhibition of its synthesis, and its reversal; applications in research and therapy. Pharmacol Ther 1991;51:155–194. [PubMed: 1784629]

9. Estrela JM, Ortega A, Obrador E. Glutathione in cancer biology and therapy. Crit Rev Clin Lab Sci 2006;43:143–181. [PubMed: 16517421]

10. Mena S, Benlloch M, Ortega A, Carretero J, Obrador E, Asensi M, Petschen I, Brown BD, Estrela JM. Bcl-2 and glutathione depletion sensitizes B16 melanoma to combination therapy and eliminates metastatic disease. Clin Cancer Res 2007;13:2658–2666. [PubMed: 17473197]

11. Wachsberger P, Burd R, Dicker AP. Tumor response to ionizing radiation combined with antiangiogenesis or vascular targeting agents: exploring mechanisms of interaction. Clin Cancer Res 2003;9:1957–1971. [PubMed: 12796357]

12. Thariat J, Yildirim G, Mason KA, Garden AS, Milas L, Ang KK. Combination of radiotherapy with EGFR antagonists for head and neck carcinoma. Int J Clin Oncol 2007;12:99–110. [PubMed: 17443277]

13. Cao Q, Cai W, Li T, Yang Y, Chen K, Xing L, Chen X. Combination of integrin siRNA and irradiation for breast cancer therapy. Biochem Biophys Res Commun 2006;351:726–732. [PubMed: 17087916]

14. Roa W, Chen H, Alexander A, Gulavita S, Thng J, Sun XJ, Petruk K, Moore R. Enhancement of radiation sensitivity with BH3I-1 in non-small cell lung cancer. Clin Invest Med 2005;28:55–63. [PubMed: 15909480]

15. Wiedenmann N, Koto M, Raju U, Milas L, Mason KA. Modulation of tumor radiation response with G3139, a bcl-2 antisense oligonucleotide. Invest New Drugs 2007;25:411–416. [PubMed: 17492397]

16. Hayashi S, Hatashita M, Matsumoto H, Shioura H, Kitai R, Kano E. Enhancement of radiosensitivity by topoisomerase II inhibitor, amrubicin and amrubicinol, in human lung adenocarcinoma A549 cells and kinetics of apoptosis and necrosis induction. Int J Mol Med 2006;18:909–915. [PubMed: 17016621]

17. Brunner TB, Hahn SM, McKenna WG, Bernhard EJ. Radiation sensitization by inhibition of activated Ras. Strahlenther Onkol 2004;180:731–740. [PubMed: 15549191]

18. Haffty BG, Glazer PM. Molecular markers in clinical radiation oncology. Oncogene 2003;22:5915–5925. [PubMed: 12947398]

19. Baker MA, Hagner BA. Diamide induced shift in protein and glutathione thiol: disulfide status delays DNA rejoining after X-irradiation of human cancer cells. Biochim Biophys Acta 1990;1037:39–47. [PubMed: 2294969]

20. Bump EA, Jacobs GP, Lee WW, Brown JM. Radiosensitization by diamide analogs and arsenicals. Int J Radiat Oncol Biol Phys 1986;12:1533–1535. [PubMed: 3759577]

21. Biaglow JE, Ayene IS, Koch CJ, Donahue J, Stamato TD, Mieyal JJ, Tuttle SW. Radiation response of cells during altered protein thiol redox. Radiat Res 2003;159:484–494. [PubMed: 12643793]

22. Held KD, Epp ER, Clark EP, Biaglow JE. Effect of dimethyl fumarate on the radiation sensitivity of mammalian cells in vitro. Radiat Res 1988;115:495–502. [PubMed: 3174933]

23. Biaglow JE, Ayene IS, Tuttle SW, Koch CJ, Donahue J, Mieyal JJ. Role of Vicinal Protein Thiols in Radiation and Cytotoxic Responses. Radiat Res 2006;165:307–317. [PubMed: 16494519]

24. Fojo T, Bates S. Strategies for reversing drug resistance. Oncogene 2003;22:7512–7523. [PubMed: 14576855]

25. Louie KG, Behrens BC, Kinsella TJ, Hamilton TC, Grotzinger KR, Mckoy WM, Winker MA, Ozols RF. Radiation survival parameters of antineoplastic drug-sensitive and –resistant human ovarian cancer cell lines and their modification by buthionie sulfoximine. Cancer Res 1985;45:2110–2115. [PubMed: 3986765]

26. Lippitz BE, Halperin EC, Griffith OW, Colvin OM, Honore G, Ostertag CB, Bigner DD, Friedman HS. L-buthionine-sulfoximine-mediated radiosensitization in experimental interstitial radiotherapy of intracerebral D-54 MG glioma xenografts in athymic mice. Neurosurgery 1990;26:255–260. [PubMed: 2308673]

27. Britten RA, Warenius HM, White R, Peacock J. BSO-induced reduction of glutathione levels increases the cellular radiosensitivity of drug-resistant human tumor cells. Int J Radiat Oncol Biol Phys 1992;22:769–772. [PubMed: 1544851]

28. Skov KA, MacPhail HS. Effect of BSO on the radiation response at low (0–4 Gy) doses. Int J Radiat Oncol Biol Phys 1992;22:533–536. [PubMed: 1346532]

29. Leung SW, Mitchell JB, al-Nabulsi I, Friedman N, Newsome J, Belldegrun A, Kasid U. Effect of L-buthionine sulfoximine on the radiation response of human renal carcinoma cell lines. Cancer 1993;71:2276–2285. [PubMed: 8095848]

30. Chattopadhyay A, Deb S, Chatterjee A. Modulation of the clastogenic activity of gamma-irradiation in buthionine sulphoximine-mediated glutathione depleted mammalian cells. Int J Radiat Biol 1999;75:1283–1291. [PubMed: 10549605]

31. Dolphine, D.; Avramovic, O.; Poulson, R. Glutathione: Chemical, Biochemical and medical Aspects, Part A. 1989.

32. Kassahun K, Jochheim CM, Baillie TA. Effect of carbamate thioester derivatives of methyl- and 2-chloroethyl isocyanate on glutathione levels and glutathione reductase activity in isolated rat hepatocytes. Biochem Pharmacol 1994;48:587–594. [PubMed: 8068046]

33. Cereser C, Boget S, Parvaz P, Revo lA. Thiram-induced cytotoxicity is accompanied by a rapid and drastic oxidation of reduced glutathione with consecutive lipid peroxidation and cell death. Toxicology 2001;163:153–162. [PubMed: 11516525]

34. Coleman MC, Asbury CR, Daniels D, Du J, Aykin-Burns N, Smith BJ, Li L, Spitz DR, Cullen JJ. 2-deoxy-D-glucose causes cytotoxicity, oxidative stress, and radiosensitization in pancreatic cancer. Free Radic Biol Med 2008;44:322–331. [PubMed: 18215740]

35. Aon MA, Cortassa S, Maack C, O'Rourke B. Sequential opening of mitochondrial ion channels as a function of glutathione redox thiol status. J Biol Chem 2007;282:21889–21900. [PubMed: 17540766]

36. Gilbert HF. Thiol/disulfide exchange equilibria and disulfide bond stability. Methods Enzymol 1995;251:8–28. [PubMed: 7651233]

37. Seefeldt T, Zhao Y, Chen W, et al. Characterization of a novel dithiocarbamate glutathione reductase inhibitor and its use as a tool to modulate intracellular glutathione. J Biol Chem 2009;284:2729–2737. [PubMed: 19049979]

38. Berridge MV, Tan AS. Characterization of the cellular reduction of 3-(4,5-dimethylthiazol-2-yl)-2,5-diphenyltetrazolium bromide (MTT): subcellular localization, substrate dependence, and involvement of mitochondrial electron transport in MTT reduction. Arch Biochem Biophys 1993;303:474–482. [PubMed: 8390225]

39. Momparler RL. In vitro systems for evaluation of combination chemotherapy. Pharmac Ther 1980;8:21–35.

40. Seefeldt T, Dwivedi C, Peitz G, Carlson L, Herman J, Zhang Z, Guan X. 2-Acetylamino-3-[4-(2-acetylamino-2-carboxy-ethylsulfanylcarbonylamino)phenyl-carbamoylsulfanyl]propionic acid and its derivatives as a novel class of glutathione reductase inhibitors. J Med Chem 2005;48:5224–5231. [PubMed: 16078841]

41. Guan X, Hoffman B, Dwivedi C, Matthees DP. A Simultaneous Liquid Chromatography/Mass Spectrometric Assay of Glutathione, Cysteine, Homocysteine and Their Disulfides in Biological Samples. J Pharm Biomed Anal 2003;31:251–261. [PubMed: 12609664]

42. Chen W, Zhao Y, Seefeldt T, Guan X. Determination of thiols and disulfides via HPLC quantification of 5-thio-2-nitrobenzoic acid. J Pharm Biomed Anal 2008;48:1375–1380. [PubMed: 18926658]

43. Jones DP. Redox potential of GSH/GSSG couple: assay and biological significance . Methods Enzymol 2002;348:93–112. [PubMed: 11885298]

44. Schirmer, RH.; Krauth-Siegel, RL. Glutathione Reductase. In: Dolphin, D.; Poulson, R.; Avramovic, O., editors. Part A Glutathione, Chemical, Biochemical, and Medical Aspects. Vol. III. New York: Wiley; 1989. p. 553-596.

45. FitzGerald GB, Bauman C, Hussoin MS, Wick MM. 2,4-Dihydroxybenzylamine: a specific inhibitor of glutathione reductase. Biochem Pharmacol 1991;41:185–190. [PubMed: 1989629]

46. Oertel S, Krempien R, Lindel K, Zabel A, Milker-Zabel S, Bischof M, Lipson KE, Peschke P, Debus J, Abdollahi A, Huber PE. Human glioblastoma and carcinoma xenograft tumors treated by combined radiation and imatinib (Gleevec). Strahlenther Onkol 2006;182:400–407. [PubMed: 16826359]

47. Balcer-Kubiczek EK, Attarpour M, Edelman MJ. The synergistic effect of dimethylamino benzoylphenylurea (NSC #639829) and X-irradiation on human lung carcinoma cell lines. Cancer Chemother Pharmacol 2007;59:781–787. [PubMed: 16957930]

48. Shrieve DC, Denekamp J, Minchinton AI. Effects of glutathione depletion by buthionine sulfoxime on radiosensitization by oxygen and misonidazole in vitro. Radiat Res 1985;102:283–294. [PubMed: 4070545]

49. Bailey HH, Ripple G, Tutsch KD, et al. Phase I study of continuous-infusion L-S, R-buthionine sulfoximine with intravenous melphalan. J Natl Cancer Inst 1997;89:1789–1796. [PubMed: 9392620]
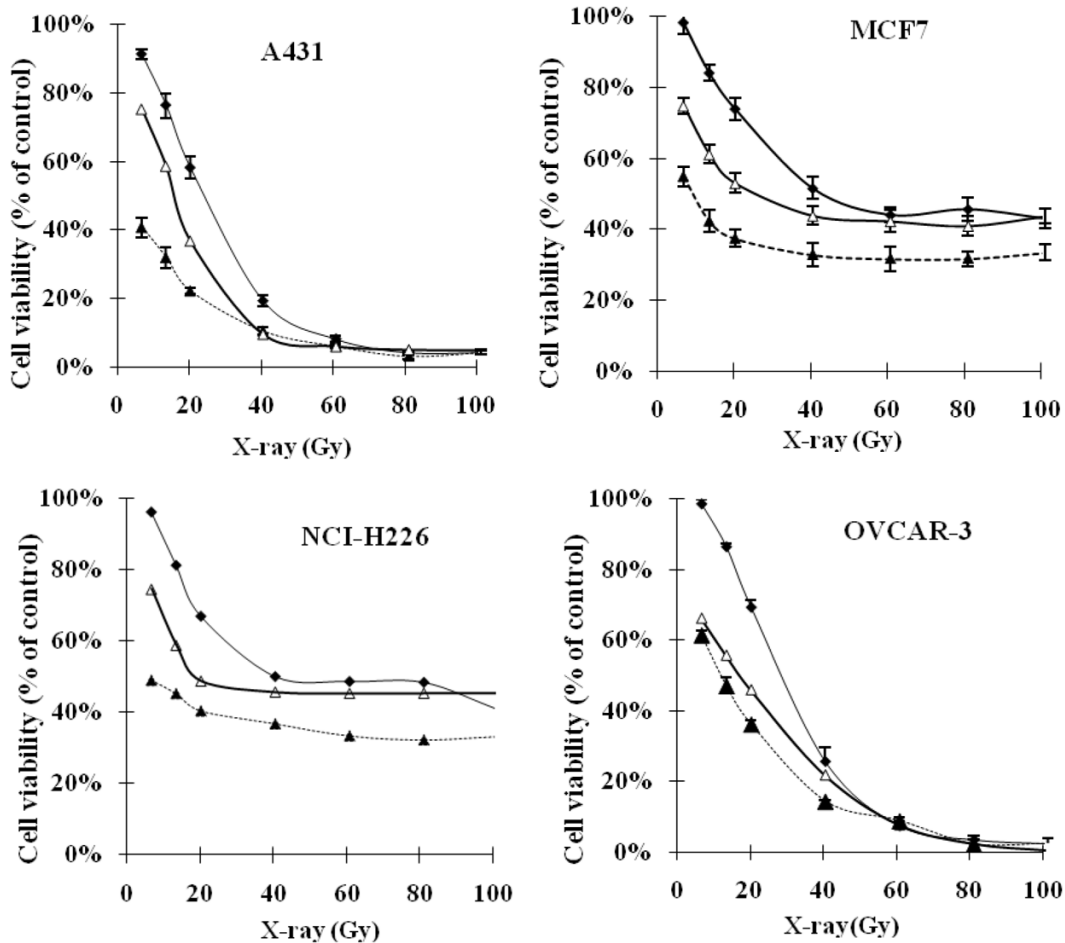
Figure 1.
The effect of 2-AAPA or BSO on the dose response curve of X-ray with A431, MCF7, NCI-H226, and OVCAR-3 cell lines (-◆-: radiation alone; -△-: BSO + radiation; -▲-: 2-AAPA + radiation;. Cells pretreated with 2-AAPA (2h) or BSO (50 μM, 24h) followed by X-ray irradiation as described in the Materials and Methods. The data are presented as percentage of the control where cells were treated with no radiation, no 2-AAPA and no BSO. The cell viability for the control was > 95%. The data are expressed as the means ± S.D. of three independent experiments.
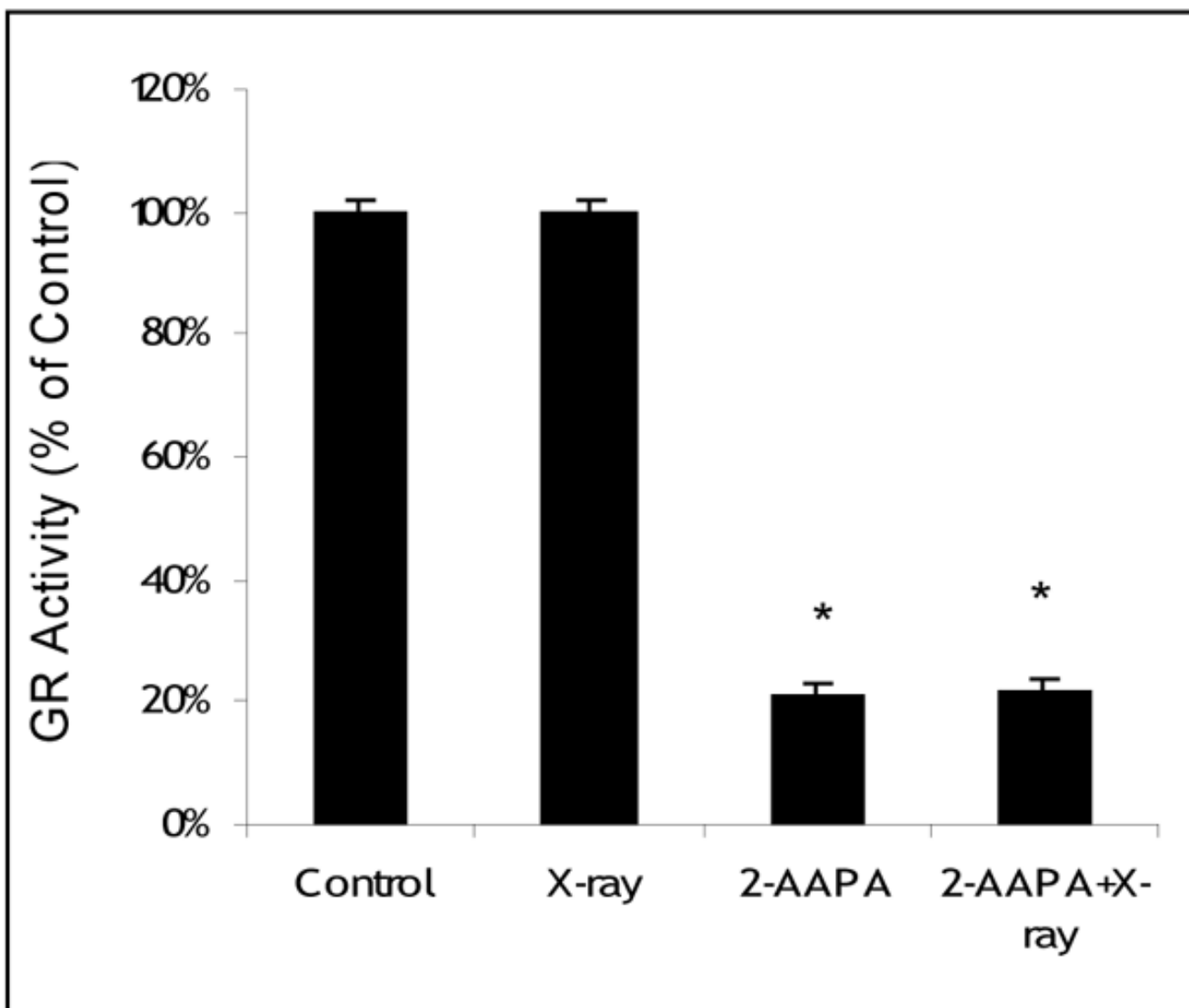
Figure 2.
GR activity in OVCAR-3 cells treated with 2-AAPA and/or X-ray. Cells were treated with 2-AAPA (50 µM, 2h), X-ray (13.5 Gy), or 2-AAPA (50 µM, 2h) plus X-ray (13.5 Gy) as indicated in the Materials and Methods. The data are presented as percentage of GR activity of the control where cells were treated with no radiation, no 2-AAPA and no BSO. The cell viability for the control was > 95%. The data are expressed as the means ± S.D. of three independent experiments. * $p < 0.05$, versus control.
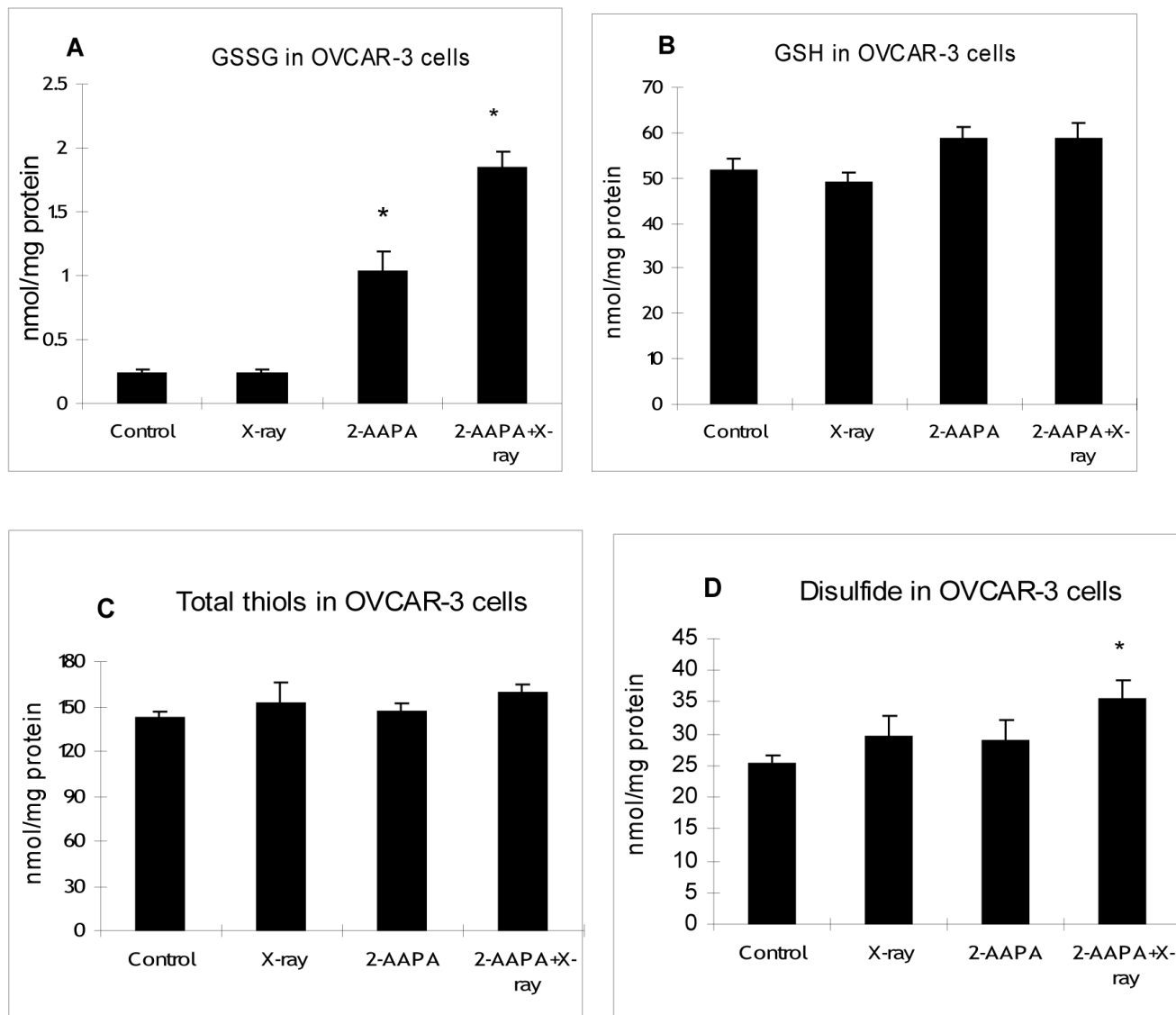
Figure 3.
GSSG (panel A), GSH (panel B), total thiols (panel C), and total disulfides (panel D) in OVCAR-3 cells treated with 2-AAPA and/or X-ray. Cells were treated with 2-AAPA (50 μM, 2h), X-ray (13.5 Gy), or 2-AAPA (50 μM, 2h) plus X-ray (13.5 Gy) as indicated in the Materials and Methods. The data are presented as the means ± S.D. of three independent experiments. *, $p < 0.05$, versus control.
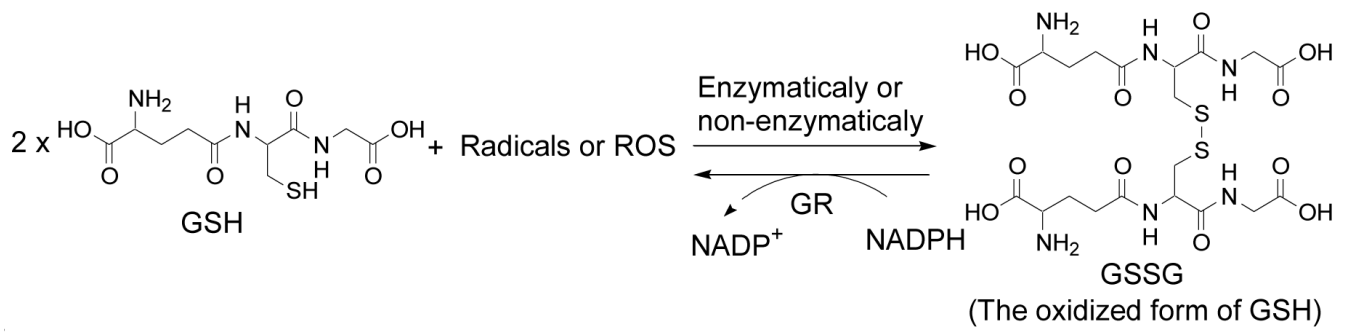
Scheme 1.
GSH being oxidized to GSSG in the presence of radicals or ROS and reduction of GSSG back
to GSH by GR.

Table 1

The effects of 2-AAPA at different concentrations on the sensitivity of cancer cell lines to X-ray radiation. Cells were pretreated with 2-AAPA for two hours followed by X-ray irradiation in a 96-well plate. The treated cells were incubated at 37°C in a humidified atmosphere of 5% CO_2 for an additional 6 days as indicated in the Materials and Methods. The X-ray dosages indicated were the dosages delivered to the 96 well plate with the lid on. The cell viability of the control was >95%. Calculation of expected cell survival rates (S_{exp}) and synergistic effects followed formulas provided in the Materials and Methods: S_{exp} = the product of the cell survival rates of 2-AAPA alone and X-ray alone; Calculated synergistic effect = $S_{exp} - S_{obs}$ where S_{obs} is the observed cell survival rate. The data are derived from three independent experiments and presented as the means ± S.D.

A

Cell line	A431		
Drug combination[*]	S_{obs} (% of control)	S_{exp} (% of control)	Calculated Synergistic effect
55 µM+X-ray (13.5 Gy)	31.9±2.1%	43.7±2.0%	11.8±1.9%
50 µM+X-ray (13.5 Gy)	46.6±2.4%	54.5±2.1%	7.9±1.9%
35 µM+X-ray (13.5 Gy)	59.9±2.1%	64.2±2.7%	4.3±1.1%
25 µM+X-ray (13.5 Gy)	62.3±1.9%	66.5±2.3%	4.2±2.0%

B

Cell line	MCF7		
Drug combination[*]	S_{obs} (% of control)	S_{exp} (% of control)	Calculated Synergistic effect
60 µM+X- ray (13.5 Gy)	42.1±2.2%	53.6±2.2%	11.5±2.4%
50 µM+X- ray (13.5 Gy)	61.1±2.1%	67.5±2.3%	6.4±2.0%
35 µM+X- ray (13.5 Gy)	66.8±2.3%	71.3±2.1%	4.5±1.9%
25 µM+X- ray (13.5 Gy)	72.3±2.1%	74.3±1.3%	2.0±1.6%

C

Cell line	NCI-H226		
Drug combination[*]	S_{obs} (% of control)	S_{exp} (% of control)	Calculated Synergistic effect
60 µM+X- ray (6.75 Gy)	47.7±2.2%	59.2±2.3%	11.5±2.3%
50 µM+X- ray (6.75 Gy)	70.1±2.0%	78.0±2.1%	7.9±2.1%
35 µM+X- ray(6.75 Gy)	83.5±2.1%	86.6±1.4%	3.1±2.9%
25 µM+X- ray (6.75 Gy)	84.9±2.4%	88.6±3.1%	3.7±1.8%

D

Cell line	OVCAR-3		
Drug combination[*]	S_{obs} (% of control)	S_{exp} (% of control)	Calculated Synergistic effect
50 µM+X- ray (13.5 Gy)	47.0±1.9%	63.7±2.4%	16.7±1.6%
35 µM+X- ray (13.5 Gy)	60.4±2.4%	69.7±3.1%	9.3±1.8%
25 µM+X- ray (13.5 Gy)	70.3±2.0%	76.2±2.9%	5.9±2.1%
15 µM+X- ray (13.5 Gy)	75.1±1.9%	79.2±2.1%	4.1±2.3%

[*] The cell survival rates were 60.5±2.3%, 75.5±2.1%, 88.9±2.0%, and 92.1±1.4% for 2-AAPA alone at 55 µM, 50 µM, 35 µM, and 25 µM respectively. The cell survival rate for X-ray alone (13.5 Gy) was 72.2±1.8%.

[*] The cell survival rates were 67.9±2.4%, 85.5±2.0%, 90.3±2.2%, and 94.2±1.8%for 2-AAPA alone at 60 µM, 50 µM, 35 µM, and 25 µM respectively. The cell survival rate for X-ray alone (13.5 Gy) was 78.9±2.5%.

[*] The cell survival rates were 60.5±2.2%, 79.5±2.4%, 88.3±2.1%, 90.3±2.5%for 2-AAPA alone at 60 µM, 50 µM, 35 µM, and 25 µM respectively. The cell survival rate for X-ray alone (6.75 Gy) was 98.1±1.5%.

*The cell survival rates were 75.4±2.2%, 82.5±2.0%, 90.2±2.3% and 93.8±1.2% for 2-AAPA alone at 60 μM, 50 μM, 35 μM, and 25 μM respectively. The cell survival rate for X-ray alone (13.5 Gy) was 84.5±1.9%.

Table 2

The effects of 2-AAPA on the sensitivity of cancer cells to X-ray radiation. Cells were pretreated with 2-AAPA for two hours followed by X-ray irradiation in a 96-well plate. The treated cells were incubated at 37°C in a humidified atmosphere of 5% CO_2 for an additional 6 days as indicated in the Materials and Methods. The concentrations of 2-AAPA employed were 55 µM, 60 µM, 60 µM, and 50 µM respectively for A431, MCF7, NCI-H226 and OVCAR-3 cells. At these concentrations, 2-AAPA alone produced cell viability of 60.5 ±2.3%, 67.9±2.4%, 60.5±2.2% and 75.4±2.2% respectively for A431, MCF7, NCI-H226 and OVCAR-3. The X-ray dosages indicated were the dosages delivered to the 96 well plate with the lid on. The cell viability of the control was >95%. Calculation of expected cell survival rates and synergistic effects followed formulas provided in the Materials and Methods: S_{exp} = the product of the cell survival rates of 2-AAPA alone and X-ray alone; Calculated synergistic effect = $S_{exp} - S_{obs}$ where S_{obs} is the observed cell survival rate. The data are derived from three independent experiments and presented as the means ± S.D.

A431

Cell line			
X-ray (Gy)	Observed cell survival (% of control)	Expected cell survival (% of control)	Calculated Synergistic effect
6.75	40.8±1.9%	52.3±2.1%	11.5±2.1%
13.50	31.9±2.1%	43.7±2.2%	11.8±1.9%
20.25	22.2±2.0%	33.3±1.9%	11.1±3.2%
40.50	10.5±1.7%	11.0±1.8%	0.5±0.2%

NCI-H226

Cell line			
X-ray (Gy)	Observed cell survival (% of control)	Calculated cell survival (% of control)	Synergistic effect
6.75	47.7±2.1%	59.2±2.1%	11.5±2.3%
13.50	43.4±1.9%	50.1±1.9%	6.7±1.2%
20.25	40.6±2.2%	41.2±2.0%	0.6±0.3%
40.50	36.3±2.0%	36.6±2.4%	0.3±0.4%

MCF7

Observed cell survival (% of control)	Expected cell survival (% of control)	Calculated Synergistic effect
52.1±2.4%	62.6±2.1%	10.5±2.2%
42.1±1.9%	53.6±2.0%	11.5±2.4%
36.2±3.0%	47.1±2.2%	10.9±1.8%
31.2±1.9%	32.9±2.3%	1.7±0.4%

OVCAR-3

Observed cell survival (% of control)	Calculated cell survival (% of control)	Synergistic effect
61.3±2.2%	72.6±2.3%	11.3±1.8%
47.0±2.1%	63.7±2.1%	16.7±1.6%
36.2±1.2%	51.1±1.9%	14.9±2.3%
14.4±1.8%	19.0±2.0%	4.6±0.9%

Table 3

The effects of BSO on the sensitivity of cancer cells to X-ray radiation. Cells were pretreated with BSO (50 μM) for 24 hours followed by X-ray irradiation in a 96-well plate. The treated cells were incubated at 37°C in a humidified atmosphere of 5% CO_2 for an additional 5 days as indicated in the Materials and Methods. BSO (50 μM) alone produced cell viability of 86.3±2.3%, 90.2±1.9%, 90.3±2.3% and 90.9±3.0% respectively for A431, MCF7, NCI-H226 and OVCAR-3. The X-ray dosages indicated were the dosages delivered to the 96 well plate with the lid on. The cell viability of the control was >95%. Calculation of expected cell survival rates and synergistic effects followed formulas provided in the Materials and Methods: S_{exp} = the product of the cell survival rates of 2-AAPA alone and X-ray alone; Calculated synergistic effect = $S_{exp} - S_{obs}$ where S_{obs} is the observed cell survival rate. The data are derived from three independent experiments and presented as the means ± S.D.

Cell line	A431			MCF7		
X-ray (Gy)	Observed cell survival (% of control)	Calculated cell survival (% of control)	Synergistic effect	Observed cell survival (% of control)	Calculated cell survival (% of control)	Synergistic effect
6.75	75.4±2.1%	82.1±2.2%	6.7±1.4%	74.9±2.2%	88.7±2.3%	13.8±1.5%
13.50	58.8±1.9%	67.3±2.2%	8.5±1.8%	61.2±2.3%	75.9±1.9%	14.7±1.2%
20.25	37.0±2.0%	52.3±1.9%	15.3±2.1%	53.1±2.1%	66.8±2.3%	13.7±2.1%
40.50	9.8±1.9%	17.4±1.8%	7.6±2.1%	43.9±1.9%	46.6±2.1%	2.7±0.3%
Cell line	NCI-H226			OVCAR-3		
X-ray (Gy)	Observed cell survival (% of control)	Calculated cell survival (% of control)	Synergistic effect	Observed cell survival (% of control)	Calculated cell survival (% of control)	Synergistic effect
6.75	74.7±2.3%	86.9±2.1%	12.2±1.4%	66.2±2.3%	88.6±2.3%	22.4±2.1%
13.50	58.9±2.0%	73.4±1.9%	14.5±1.5%	55.7±2.0%	78.1±2.4%	22.4±2.3%
20.25	48.9±2.4%	60.5±2.3%	11.6±2.1%	45.9±2.2%	62.2±2.1%	16.3±1.8%
40.50	45.7±1.9%	46.1±2.4%	0.4±0.4%	21.8±2.3%	23.9±1.9%	2.1±0.3%